.

Nanosecond spin relaxation times in single layer graphene spin valves with hexagonal boron nitride tunnel barriers

Simranjeet Singh, Jyoti Katoch, Jinsong Xu, Cheng Tan, Tiancong Zhu, Walid Amamou, James Hone, and Roland Kawakami'

Citation: Appl. Phys. Lett. **109**, 122411 (2016); doi: 10.1063/1.4962635
View online: http://dx.doi.org/10.1063/1.4962635
View Table of Contents: http://aip.scitation.org/toc/apl/109/12
Published by the American Institute of Physics

RIGHTSLINK

APPLIED PHYSICS LETTERS **109**, 122411 (2016)

Nanosecond spin relaxation times in single layer graphene spin valves with hexagonal boron nitride tunnel barriers

Simranjeet Singh,[1] Jyoti Katoch,[1] Jinsong Xu,[1] Cheng Tan,[2] Tiancong Zhu,[1] Walid Amamou,[3] James Hone,[2] and Roland Kawakami[1,3,a)]
[1]*Department of Physics, The Ohio State University, Columbus, Ohio 43210, USA*
[2]*Mechanical Engineering Department, Columbia University, New York, New York 10027, USA*
[3]*Program of Materials Science and Engineering, University of California, Riverside, California 92521, USA*

(Received 11 June 2016; accepted 26 August 2016; published online 22 September 2016)

We present an experimental study of spin transport in single layer graphene using atomic sheets of hexagonal boron nitride (h-BN) as a tunnel barrier for spin injection. While h-BN is expected to be favorable for spin injection, previous experimental studies have been unable to achieve spin relaxation times in the nanosecond regime, suggesting potential problems originating from the contacts. Here, we investigate spin relaxation in graphene spin valves with h-BN barriers and observe room temperature spin lifetimes in excess of a nanosecond, which provides experimental confirmation that h-BN is indeed a good barrier material for spin injection into graphene. By carrying out measurements with different thicknesses of h-BN, we show that few layer h-BN is a better choice than monolayer for achieving high non-local spin signals and longer spin relaxation times in graphene. *Published by AIP Publishing*. [http://dx.doi.org/10.1063/1.4962635]

Graphene is a promising spin channel material for next generation spintronic devices due to the experimental demonstration of long spin diffusion lengths at room temperature[1–3] and theoretical predictions of long spin relaxation times[4,5] arising from the weak spin-orbit and hyperfine couplings.[5,6] However, experimentally measured spin relaxation times[1–3,7,8] in graphene are orders of magnitude shorter than theoretically predicted.[4,5] In graphene spin valves, the tunnel barrier plays a crucial role for spin injection by circumventing the problem of impedance mismatch[9] between graphene and the ferromagnetic electrodes. As demonstrated by Han *et al.*,[8] high quality tunnel barriers are critical for obtaining higher spin relaxation times (τ_s) in graphene because barriers with pinholes or rough surface morphology can cause additional contact-induced spin relaxation, which has received a great deal of interest recently.[10–14] As opposed to growing oxide tunnel barriers on graphene, a thin insulating two-dimensional (2D) van der Waals material can also be used as a tunnel barrier. A particular material of interest is single (or few) layer h-BN because of its various suitable properties:[15] large energy band gap $\sim$5.97 eV, high crystallinity, spin filtering,[16] absence of pinholes and dangling bonds, atomic lattice similar to graphene, and chemical stability at ambient conditions. In addition, atomically clean vertical heterostructures of h-BN/graphene can be mechanically assembled using polymer-based transfer techniques.[17,18] The first experimental report demonstrating spin injection into graphene using a monolayer h-BN tunnel barrier showed τ_s less than 100 ps.[19] This was followed by the work of Kamalakar *et al.*[20,21] and Fu *et al.*,[22] which used chemically grown h-BN barriers, yielding $\tau_s \sim 500$ ps. Another recent study using an encapsulated geometry[23] with graphene sandwiched between a thick bottom layer of h-BN and a monolayer of h-BN on top showed τ_s less than 200 ps. As evident from these studies, graphene spin valve devices with h-BN tunnel barriers have yielded relatively small values for τ_s (<1 ns) that are comparable with or lower than the values obtained using oxide barriers. Thus, it is worthwhile to ask: are h-BN tunnel barriers compatible with longer spin lifetimes in graphene?

In this letter, we perform spin transport in single layer graphene spin valve devices with h-BN tunnel barriers and observe spin relaxation times exceeding a nanosecond at room temperature, the highest values achieved so far for devices employing h-BN tunnel barriers. In addition, we investigate the thickness dependent characteristics of the h-BN tunnel barriers and find that few layer h-BN, rather than monolayer, is required to observe large non-local spin signals and longer spin relaxation times in graphene. Our work establishes the effectiveness of ultrathin h-BN as a high quality tunnel barrier for spin injection into graphene, which is a crucial step towards realizing high performance spintronic devices based completely on ultrathin van der Waals materials.

For making h-BN/graphene interfaces, thin h-BN flakes are exfoliated from bulk crystals (HQ graphene) on a 90 nm SiO_2/Si wafer, and the thickness of h-BN is confirmed by atomic force microscopy (AFM). On a separate 300 nm SiO_2/Si substrate, Kish graphite is exfoliated to obtain single layer graphene, confirmed by Raman spectroscopy. Figure 1(a) shows the Raman spectra of the graphene used in the h-BN/graphene heterostructures. Thin h-BN is transferred onto single layer graphene using a process similar to Zomer *et al.*[24] In short, a polydimethylsiloxane (PDMS) stamp coated with polycarbonate (PC) polymer is attached to a glass slide and is brought in contact with an exfoliated h-BN flake. Next, the PC film is heated to 70 °C to pick-up the h-BN flake from the SiO_2 surface. Once the h-BN is on the PC film, it is optically aligned to the desired graphene flake and then the PC film is melted onto the graphene flake's substrate at 150 °C. The PC film is removed by dissolving it in chloroform for 30 min. Afterward, the h-BN/graphene heterostructure is cleaned by

a)Author to whom correspondence should be addressed. Electronic mail: kawakami.15@osu.edu

RIGHTSLINK

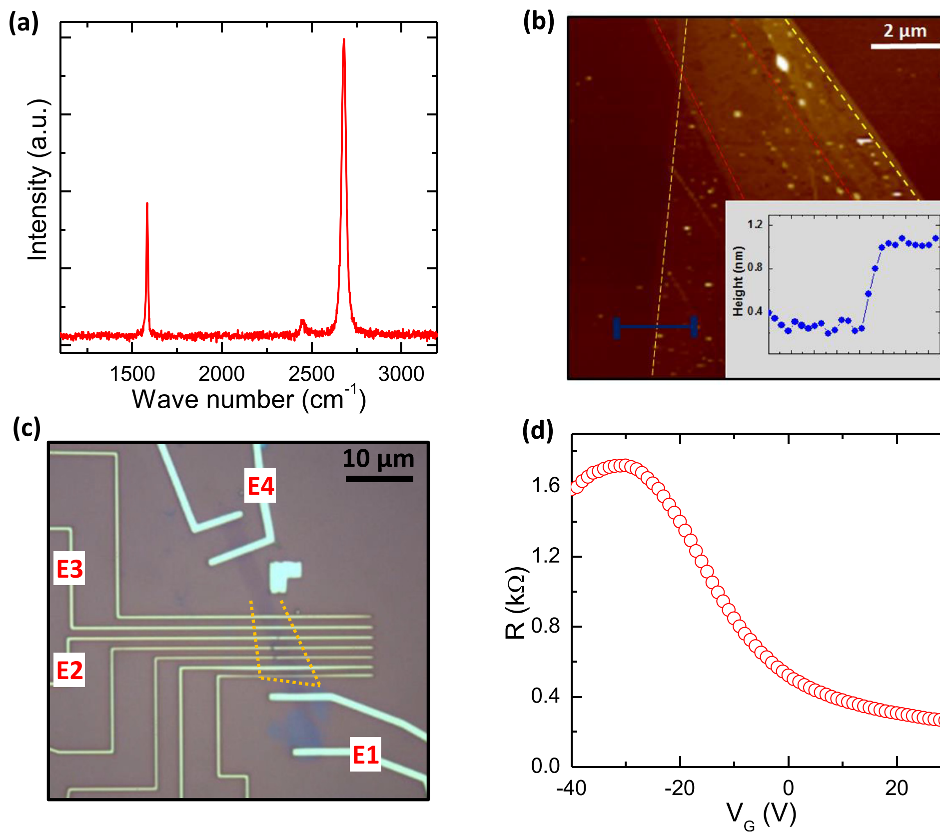

FIG. 1. (a) Raman spectra confirming single layer graphene. (b) Atomic force microscopy of the h-BN/graphene stack (before defining the ferromagnetic electrodes) showing the topography of graphene and thin h-BN. The boundaries of the graphene and top h-BN are highlighted by red and yellow dotted lines, respectively. The thickness of the h-BN is ∼0.85 nm (2–3 monolayers) and the step height of h-BN is shown in the inset. (c) The optical image of the completed device, with different electrodes used for the measurements labeled for convenience. The h-BN flake boundary is depicted by yellow dotted lines. (d) The gate dependent resistance of the graphene channel measured at room temperature.

annealing in H_2/Ar forming gas at 350 °C for 3 h. Figure 1(c) shows the surface topography of the measured h-BN/graphene stack, where the top h-BN and the graphene are outlined by yellow and red dashed lines, respectively. The measured thickness of the h-BN is 0.85 nm, as shown by the step height in the inset of Figure 1(b), which corresponds to 2–3 layers of h-BN[25] (monolayer thickness is ∼0.34 nm). Although there are few small bubbles trapped between the graphene and h-BN, there are still large bubble-free regions that can be used for the cobalt contacts. Figure 1(c) shows the optical microscope image of the measured spin valve device, in which yellow dotted lines highlight the boundary of the h-BN tunnel barrier. In order to electrically characterize the graphene sheet, we measure the four-probe resistance (at room temperature) of graphene as a function of back gate voltage (V_G) applied to the degenerately doped Si substrate (Figure 1(d)). An electron mobility of 4000 cm^2/V s is extracted from the slope of the graphene conductivity versus gate voltage scan.[26] The contact resistance of the electrodes with h-BN barrier is measured using a three-probe measurement configuration.[8] The zero bias contact resistance of the electrodes varies from a few kilo-Ohms (kΩ) to hundreds of kΩ depending on the thickness of the h-BN. This will be discussed in detail later.

We begin by discussing the spin transport measurements carried out at room temperature. For the data presented here, the graphene channel length is 1.5 μm and width is 2.5 μm. The contact resistances of the injector (E2; Fig. 1(c)) and detector (E3; Fig. 1(c)) electrodes are 42 kΩ and 6 kΩ, respectively. The temperature dependence and bias dependence of the contact resistances indicate tunneling behavior (see supplementary material). To measure the non-local magnetoresistance (MR) signal, we perform low frequency ac measurements using a current excitation of 1 μA rms. As shown by the schematic in the inset to Figure 2(a), spin injection current is applied between the electrodes labeled E1 and E2, and a non-local voltage signal is measured using the electrodes labeled E3 and E4. An external magnetic field is swept in the plane of the graphene device (along the electrode's length), and a non-local voltage signal is recorded as a function of the applied magnetic field. To obtain the non-local resistance (R_{NL}), the voltage signal is divided by the magnitude of applied current (1 μA). Figure 2(a) shows the observed non-local MR signal at room temperature, where black circles are data recorded by a sweep in increasing magnetic field. At ∼20 mT, we see an abrupt change in R_{NL} when one of the magnetizations reverses to create an antiparallel alignment of the injector and detector magnetizations (arrows indicate the relative alignment of the magnetizations throughout the magnetic field sweeps). This is the hallmark of spin transport from injector to detector. With further increase of the magnetic field, the resistance signal again changes back to the original value due to the alignment of the injector and detector magnetizations back to a parallel configuration. Also shown in Figure 2(a) is the MR signal when sweeping with a decreasing magnetic field (blue circles). The magnitude of the measured MR signal (ΔR_{NL}) is defined as the difference of R_{NL} between the parallel and antiparallel configurations, and is approximately 4 Ω for the measured device at $V_G = +10$ V. We also measure the gate dependence of the non-local MR on the applied gate voltage, which tunes the polarity and density of the charge carriers and observe ΔR_{NL} as large as 5 Ω over the measured gate voltage range (data shown in the supplementary Figure S2b).

RIGHTSLINK

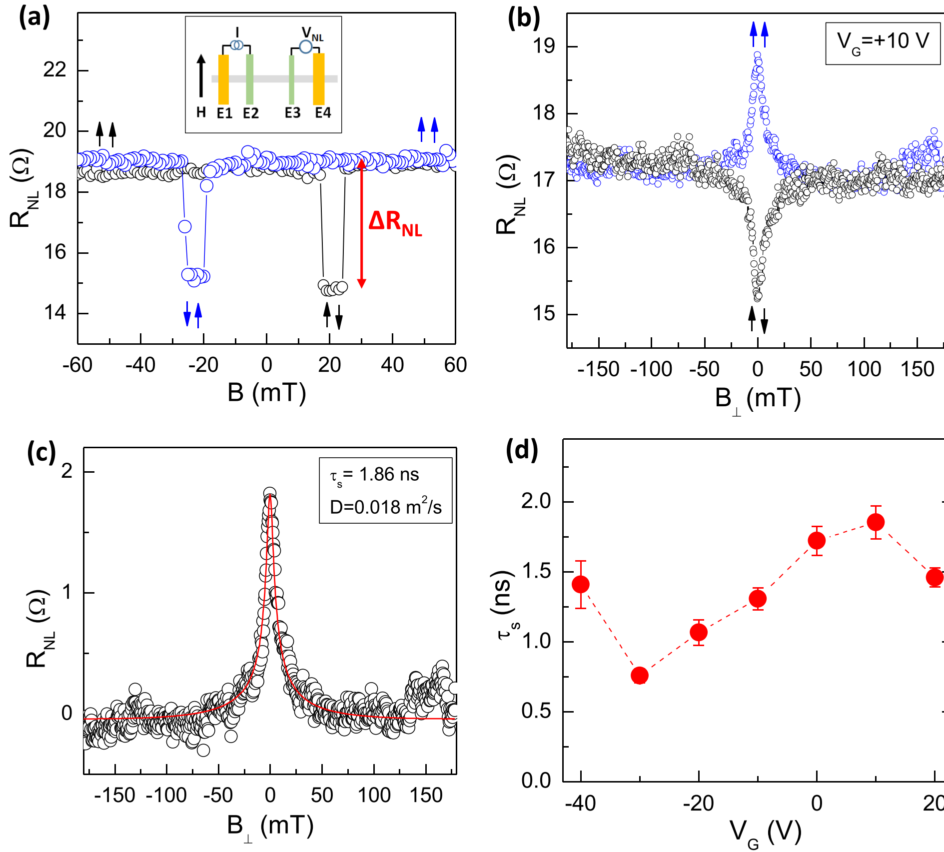

FIG. 2. Spin transport in single layer graphene using few layer h-BN tunnel barriers, measured at room temperature. (a) Non-local magneto-resistance (MR) signal measured in a graphene spin valve with h-BN tunnel barriers using E2 and E3 as injector and detector electrodes, respectively, at room temperature. The blue and black arrows represent the relative magnetization direction of injector and detector electrodes. ΔR_{NL} is the magnitude of the MR signal. Inset: schematic of the non-local measurement configuration. (b) Non-local Hanle spin precession signal measured in parallel (blue circles) and antiparallel (black circles) configuration by applying an out of plane magnetic field. The blue and black arrows represent the relative magnetization direction of injector and detector. (c) Non-local Hanle spin precession curve (black circles) obtained by subtracting parallel and antiparallel Hanle curves from Figure 2(b). The thick red line is the fit to the data to extract the spin relaxation time (τ_s). (d) The gate dependence of the fitted spin relaxation times over a range of applied back gate voltages.

To study the spin relaxation times in the graphene channel, we perform non-local Hanle spin precession measurements at room temperature. In a typical Hanle measurement, the in-plane polarized spins precess in the graphene plane by an externally applied out of plane magnetic field. After aligning the magnetization of the injector and detector, either in a parallel or antiparallel configuration, a magnetic field is swept perpendicular to the plane of the graphene device to measure the non-local resistance signal as a function of applied magnetic field. Figure 2(b) shows the Hanle curves obtained for the graphene spin valve device measured in parallel (blue circles) and antiparallel (black circles) configuration. The measured sweeps for parallel and antiparallel configurations are subtracted to obtain the curve as shown in Figure 2(c) (black circles). In general, once the spins are injected from the ferromagnetic electrode, the spin transport in graphene can be described by majority and minority spin channels. The voltage signal measured at the detector electrode is proportional to net spin accumulation ($\boldsymbol{\mu_S}$), where $|\mu_S|$ is the difference of the electrochemical potentials of majority and minority spins and the vector points along the polarization axis. This spin accumulation in an applied magnetic field can be described by solving the steady state Bloch equation

$$D\nabla^2\boldsymbol{\mu}_s - \frac{\boldsymbol{\mu}_s}{\tau_s} + \boldsymbol{\omega_L} \times \boldsymbol{\mu}_s = 0, \tag{1}$$

where D is the diffusion constant in the graphene channel, τ_s is the spin relaxation time, $\boldsymbol{\omega_L} = g\mu_B \mathbf{B}/\hbar$ is the Larmor frequency, $g = 2$ is the gyromagnetic factor, μ_B is the Bohr magneton, $\hbar$ is the reduced Planck's constant, and $\boldsymbol{B}$ is the externally applied magnetic field. To fit the measured non-local Hanle data we use an analytical expression developed by Sosenko *et al.*[27] which is the solution to the steady state Bloch equation (Eq. (1)) in the presence of boundary conditions for the injection and absorption of spin current at the ferromagnetic electrodes

$$R_{NL}^{\pm} = \pm p_1 p_2 R_N f, \tag{2}$$

where the $\pm$ corresponds to the relative alignment of injector/detector magnetizations, p_1 and p_2 are the electrode spin polarizations, $R_N = \frac{\lambda}{W L \sigma^N}$ is the spin resistance of graphene, λ is the spin diffusion length in graphene (related to τ_s by $\lambda = \sqrt{D\tau_s}$), W is the width of the graphene, σ^N is the conductivity of graphene and

$$f = Re\left(2\left[\sqrt{1+i\omega_L\tau_s} + \frac{\lambda}{2}\left(\frac{1}{r_s} + \frac{1}{r_d}\right)\right] e^{\left(\frac{L}{\lambda}\right)\sqrt{1+i\omega_L\tau_s}} + \frac{\lambda^2}{r_s r_d} \frac{\sinh\left[\left(\frac{L}{\lambda}\right)\sqrt{1+i\omega_L\tau_s}\right]}{\sqrt{1+i\omega_L\tau_s}} \right)^{-1}. \tag{3}$$

In the function f, $r_i = \frac{R_F + R_C^i}{R_{SQ}} W$ with $i = s, d$ for the injector and detector, respectively, R_C is the contact resistance, R_{SQ} is the graphene sheet resistance, $R_F = \rho_F \lambda_F / A$ is the spin resistance of the ferromagnetic electrode material, ρ_F is the resistivity of the ferromagnet, λ_F is the spin diffusion length in the ferromagnet, and A is the area of the graphene/electrode junction.

Using Equation (2), the experimentally obtained Hanle curves can be fit using τ_s, λ, and the product p_1p_2 as fitting

RIGHTSLINK

parameters. The fit for the Hanle curve at zero gate voltage (solid red line in Figure 2(c)) yields values of $\tau_s = 1.86$ ns, $\lambda = 5.78\ \mu$m, $\sqrt{p_1 p_2} = 0.053$, and $D = 0.018\ m^2/s$. The corresponding spin injection efficiency is found to be 0.052 (see supplementary material). We also investigated the gate dependence of the spin lifetimes by measuring Hanle precession curves at different V_G and fitting each of these curves with Equation (2). Figure 2(d) shows the extracted τ_s as a function of applied gate voltages, where, for most of the applied gate voltages, τ_s exceeds 1 ns. This experimental demonstration of nanosecond spin lifetimes in graphene on SiO_2 substrates at room temperature, employing h-BN tunnel barriers, is the central result of this work. These observed nanosecond spin lifetimes are the highest values reported in the literature for a single layer graphene channel employing an h-BN tunnel barrier.[19–23] It is important to note that for van der Waals heterostructures, it is non-trivial to achieve clean interfaces,[17,28] and the impurities (or residues) at the interface can affect the electrical and spin related properties across the van der Waals heterostructures. One possible explanation for the high quality spin transport observed in our studies may be the relatively clean h-BN/graphene interface, evidenced by the flat surface topography of the heterostructure, in areas where we deposited ferromagnetic electrodes for spin injection.

We have also spin transport in graphene spin valves using monolayer h-BN[19,25] (~0.50 nm thick) tunnel barriers, in contrast to the few layer (2–3) h-BN barriers discussed so far. Here we present data using a pair of electrodes with injector and detector contact resistance of 7.7 kΩ and 3.7 kΩ, respectively. The detailed temperature dependence of the contact resistance is shown in the supplementary material. The graphene channel length is 5 μm and width is 4.9 μm. The charge carrier mobility of the graphene channel is 8000 cm^2/V s. As shown in Figure 3(c), the non-local MR signal measured at 11 K and $V_G = +10$ V exhibits a magnitude of 170 mΩ. We present data taken at low temperatures because we are unable to resolve clear MR switching at RT beyond the noise, but can observe clear MR at low temperatures. The magnitude of the MR (ΔR_{NL}) as a function of gate voltage varies from 100 mΩ to 350 mΩ (data shown in the supplementary material). Figure 3(b) shows the Hanle curve (black circles) obtained by carrying out non-local Hanle measurements at a $V_G = +10$ V. By fitting the data with Equation (2) we extract $\tau_s = 490$ ps, $\lambda = 3.8\ \mu$m, $\sqrt{p_1 p_2} = 0.023$, and $D = 0.03\ m^2/s$. Figure 3(c) shows the extracted τ_s as a function of applied gate voltage, where the inset shows the gate dependent resistance of the measured graphene channel. The spin relaxation times extracted from the Hanle curves range from 300 ps to 600 ps, which are similar to (or slightly higher than) previous studies employing monolayer h-BN tunnel barriers.[19,23] Our measurements suggest that monolayer h-BN may not be the optimal choice for efficient spin injection, while thicker h-BN allows the realization of larger MR signals and longer spin relaxation times in graphene spin valves. One of the possible reasons for higher spin relaxation times in graphene using multilayer h-BN tunnel barriers could be related to the fact that few layer h-BN (on SiO_2 substrate) is flatter,[17] i.e., less ripples in surface morphology, than single layer h-BN. This could lead to smoother growth of cobalt electrodes on multilayer h-BN and thus reduce the contact-induced spin dephasing mechanism due to the magnetostatic fringe field[29] of the ferromagnetic material. Apart from this, we also speculate that single layer h-BN is more prone to surface contaminants such as organic residues or wrinkles during the transfer process and can cause additional spin dephasing under the ferromagnet contact resulting in shorter spin relaxation times in graphene.

In order to investigate the range of h-BN thickness required to observe large MR signals and higher spin relaxation times in graphene spin valves, we have prepared different h-BN/graphene stacks with h-BN thicknesses varying from ~0.50 nm to 3.20 nm. The thicknesses of the h-BN flakes were characterized by AFM. In total, we measured six different devices with h-BN tunnel barriers. For each device with multiple ferromagnetic electrodes, the interfacial contact resistance was measured using a 3-probe configuration,[8] wherein the differential contact resistance (dV/dI) was measured as a function of dc bias current at low temperature. The dV/dI curves show a zero bias peak, as expected for a tunnel barrier. The values of zero bias dV/dI as function of the h-BN thickness are plotted in Figure 4 for all the measured electrodes. The gray dotted circle denotes the region, corresponding to

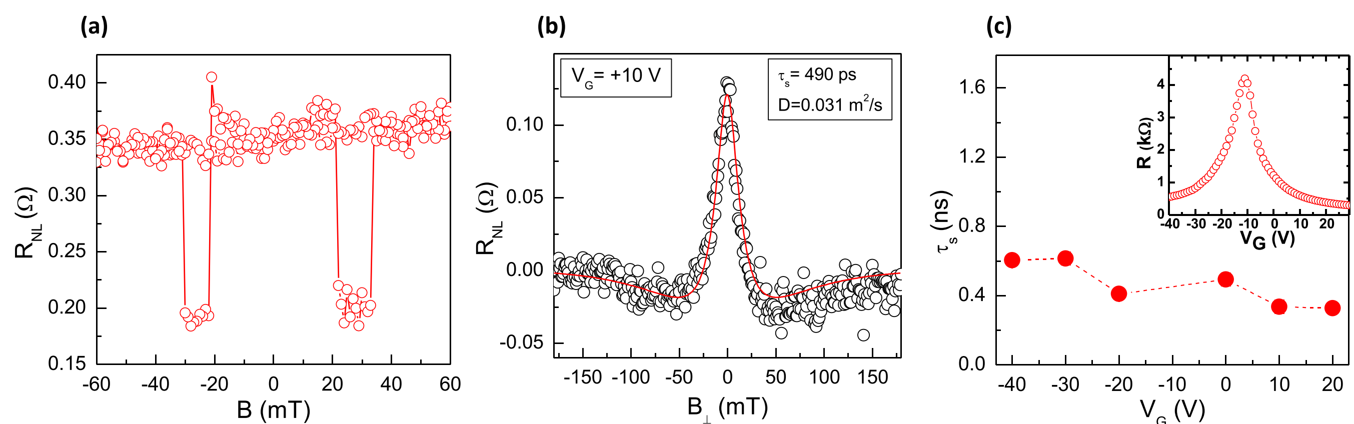

FIG. 3. Spin transport in single layer graphene using monolayer h-BN tunnel barriers, measured at 11 K. (a) Non-local magnetoresistance (MR) signal measured in a graphene spin valve using monolayer h-BN at $V_G = +10$ V. (b) Non-local Hanle signal (black circles) measured by applying an out of plane magnetic field at $V_G = +10$ V. The red line is the fitting to the data to extract spin relaxation time (τ_s). (c) The fitted spin relaxation times as function of applied back gate. Inset: graphene channel resistance as a function of gate voltage.

RIGHTSLINK Copyright Clearance Center

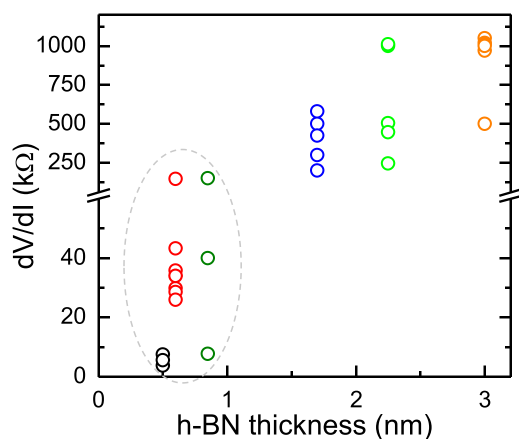

FIG. 4. Low temperature tunneling characteristics of different thickness h-BN barriers. Differential contact resistance of the electrodes (for 6 different devices) is shown as a function of AFM measured thickness of the h-BN layer. The gray circle shows the region for which we have observed MR signals.

h-BN thicknesses, for which we were able to observe MR signals. We did not observe any non-local MR signal in devices with h-BN thickness larger than 1.50 nm (∼4 monolayers of h-BN). Note that one would expect to have a small distribution of contact resistances for a given h-BN thickness, but the interfacial inhomogeneities (e.g., bubbles or organic residues) at the h-BN/graphene interface over mesoscopic size areas could give rise to the observed contact resistance distributions.

In conclusion, our experimental work demonstrates that h-BN is a high quality tunnel barrier material for spin injection into graphene, as evident from our data showing large non-local MR signals and nanosecond spin relaxation times at room temperature. Our experimental observations indicate that few layer h-BN leads in better characteristics, as opposed to monolayer h-BN, for tunnel barrier applications to achieve higher quality spin transport in graphene. More experimental studies are needed to further improve the interface quality of h-BN/graphene in order to exploit the full potential of van der Waals heterostructures for spin related physics in graphene and other 2D materials.

See supplementary material for detailed discussion and data for: temperature dependence of the interfacial contact resistances, gate dependent MR signals, and h-BN thickness dependence of the spin injection efficiency.

The authors acknowledge Elizabeth Bushong for carefully reading the manuscript. S.S., J.K., J.X., T.Z., W.A., and R.K. acknowledge support from ONR (No. N00014-14-1-0350), NRI-NSF (No. DMR-1124601), NSF (No. DMR-1310661), and C-SPIN, one of the six SRC STARnet Centers, sponsored by MARCO and DARPA. C.T. was supported by a DOD-AFOSR, NDSEG fellowship under Contract No. FA9550-11-C-0028, 32 CFR 168a. C.T. and J.H. acknowledge support from the Nanoelectronics Research Initiative (NRI) through the Institute for Nanoelectronics Discovery and Exploration (INDEX).

[1] M. H. D. Guimarães, P. J. Zomer, J. Ingla-Aynés, J. C. Brant, N. Tombros, and B. J. van Wees, Phys. Rev. Lett. **113**, 086602 (2014).
[2] M. Drögeler, F. Volmer, M. Wolter, B. Terrés, K. Watanabe, T. Taniguchi, G. Güntherodt, C. Stampfer, and B. Beschoten, Nano Lett. **14**, 6050 (2014).
[3] M. Drögeler, C. Franzen, F. Volmer, T. Pohlmann, L. Banszerus, M. Wolter, K. Watanabe, T. Taniguchi, C. Stampfer, and B. Beschoten, Nano Lett. **16**, 3533 (2016).
[4] D. Huertas-Hernando, F. Guinea, and A. Brataas, Phys. Rev. B **74**, 155426 (2006).
[5] W. Han, R. K. Kawakami, M. Gmitra, and J. Fabian, Nat. Nano **9**, 794 (2014).
[6] A. H. Castro Neto, F. Guinea, N. M. R. Peres, K. S. Novoselov, and A. K. Geim, Rev. Mod. Phys. **81**, 109 (2009).
[7] N. Tombros, C. Jozsa, M. Popinciuc, H. T. Jonkman, and B. J. van Wees, Nature **448**, 571 (2007).
[8] W. Han, K. Pi, K. M. McCreary, Y. Li, J. J. I. Wong, A. G. Swartz, and R. K. Kawakami, Phys. Rev. Lett. **105**, 167202 (2010).
[9] G. Schmidt, D. Ferrand, L. W. Molenkamp, A. T. Filip, and B. J. van Wees, Phys. Rev. B **62**, R4790 (2000).
[10] M. Popinciuc, C. Józsa, P. J. Zomer, N. Tombros, A. Veligura, H. T. Jonkman, and B. J. van Wees, Phys. Rev. B **80**, 214427 (2009).
[11] T. Maassen, I. J. Vera-Marun, M. H. D. Guimarães, and B. J. van Wees, Phys. Rev. B **86**, 235408 (2012).
[12] W. Amamou, Z. Lin, J. van Baren, S. Turkyilmaz, J. Shi, and R. K. Kawakami, APL Mater. **4**, 032503 (2016).
[13] H. Idzuchi, A. Fert, and Y. Otani, Phys. Rev. B **91**, 241407 (2015).
[14] H. Idzuchi, Y. Fukuma, S. Takahashi, S. Maekawa, and Y. Otani, Phys. Rev. B **89**, 081308 (2014).
[15] K. Watanabe, T. Taniguchi, and H. Kanda, Nat. Mater. **3**, 404 (2004).
[16] M. V. Kamalakar, A. Dankert, P. J. Kelly, and S. P. Dash, Sci. Rep. **6**, 21168 (2016).
[17] C. R. Dean, A. F. Young, I. Meric, C. Lee, L. Wang, S. Sorgenfrei, K. Watanabe, T. Taniguchi, P. Kim, K. L. Shepard, and J. Hone, Nat. Nano **5**, 722 (2010).
[18] L. Wang, I. Meric, P. Y. Huang, Q. Gao, Y. Gao, H. Tran, T. Taniguchi, K. Watanabe, L. M. Campos, D. A. Muller, J. Guo, P. Kim, J. Hone, K. L. Shepard, and C. R. Dean, Science **342**, 614 (2013).
[19] Y. Takehiro, I. Yoshihisa, M. Satoru, M. Sei, O. Masahiro, W. Kenji, T. Takashi, M. Rai, and M. Tomoki, Appl. Phys. Express **6**, 073001 (2013).
[20] M. V. Kamalakar, A. Dankert, J. Bergsten, T. Ive, and S. P. Dash, Appl. Phys. Lett. **105**, 212405 (2014).
[21] M. V. Kamalakar, A. Dankert, J. Bergsten, T. Ive, and S. P. Dash, Sci. Rep. **4**, 6146 (2014).
[22] W. Fu, P. Makk, R. Maurand, M. Bräuninger, and C. Schönenberger, J. Appl. Phys. **116**, 074306 (2014).
[23] M. Gurram, S. Omar, S. Zihlmann, P. Makk, C. Schönenberger, and B. J. van Wees, Phys. Rev. B **93**, 115441 (2016).
[24] P. J. Zomer, M. H. D. Guimarães, J. C. Brant, N. Tombros, and B. J. van Wees, Appl. Phys. Lett. **105**, 013101 (2014).
[25] G.-H. Lee, Y.-J. Yu, C. Lee, C. Dean, K. L. Shepard, P. Kim, and J. Hone, Appl. Phys. Lett. **99**, 243114 (2011).
[26] J.-H. Chen, C. Jang, S. Xiao, M. Ishigami, and M. S. Fuhrer, Nat. Nano **3**, 206 (2008).
[27] E. Sosenko, H. Wei, and V. Aji, Phys. Rev. B **89**, 245436 (2014).
[28] S. J. Haigh, A. Gholinia, R. Jalil, S. Romani, L. Britnell, D. C. Elias, K. S. Novoselov, L. A. Ponomarenko, A. K. Geim, and R. Gorbachev, Nat. Mater. **11**, 764 (2012).
[29] S. P. Dash, S. Sharma, J. C. Le Breton, J. Peiro, H. Jaffrès, J. M. George, A. Lemaître, and R. Jansen, Phys. Rev. B **84**, 054410 (2011).

RIGHTSLINK